Acta Mech 226, 1807–1813 (2015)
DOI 10.1007/s00707-014-1289-8

R. Bustamante · K. R. Rajagopal

Solutions of some boundary value problems for a new class of elastic bodies. Comparison with predictions of the classical theory of linearized elasticity: Part II. A problem with spherical symmetry

Received: 18 July 2014 / Revised: 20 October 2014 / Published online: 27 December 2014

Abstract In Part II of the paper, we study the response of a spherical annular region of the same strain limiting elastic body considered in Part I, wherein the linearized strain is a nonlinear function of the stress. We study the response of the annular region due to a normal radial inflation, and as in Part I, we find the response to be strikingly different from that of the classical linearized elastic solid.

1 Introduction

This Part II is a continuation of a study of the response of a new class of elastic bodies that were studied in Part I [1]. The motivation for studying boundary value problems within the context of this new class of elastic bodies wherein the linearized strain and the stress are related nonlinearly, that exhibit strain limiting behavior, was explained in detail in Part I of this paper (see [1]) and hence we shall not repeat them here. The class of models that is considered is a consequence of the classical linearization procedure applied to bodies defined by a response relation for the nonlinear strain, nonlinear terms of the stress, under assumption that the displacement gradients are sufficiently small so that we can ignore the nonlinearity in the Green-St. Venant strain (see Rajagopal [2–5]). In Part I of the paper, we studied two classes of boundary value problems: the first wherein a cylindrical tube was subject to telescopic shear and inflation, and the second when the tube was subject to circumferential shear, extension, and inflation. In this Part II, we consider a different class of boundary value problems, that of a spherical annulus of the class of bodies studied in Part I subject to inflation. Three types of bodies, one corresponding to a thin-walled spherical shell, the second a thick-walled spherical shell, and the third an extended body with a spherical cavity, are studied due to radial inflation. The results for the state of stress and the displacement in the annulus that are obtained are compared against the corresponding results for the classical linearized elastic model. While one can obtain an explicit exact solution in the case of the classical linearized elastic model, we are unable to do so for the nonlinear model, which has to be studied numerically using the finite element method. As in Part I, we find that the results for the nonlinear model are in conspicuously contrast to the results obtained for the classical linearized elastic model.

The organization of this part is as follows: In the next section, we introduce the kinematics, the governing equations, the response relation, and the boundary value problem. This is followed in Sect. 3 by a discussion of the problem of inflation of a sphere in detail. Results are presented for the state of stress within the annular region and the displacement of the annular region.

R. Bustamante (✉)
Departamento de Ingeniería Mecánica, Universidad de Chile, Beaucheff 850, Santiago Centro, Santiago, Chile
E-mail: rogbusta@ing.uchile.cl

K. R. Rajagopal
Department of Mechanical Engineering, University of Texas A&M, College Station TX, USA

2 Basic equations, response relations, and the definition of the boundary value problem

We shall keep our kinematical definitions to a minimum. More details can be found in the references [6,7] and [8]. Let $\mathbf{X}$, where $\mathbf{X} = \boldsymbol{\kappa}_r(X)$, denote the position of a particle X of a body $\mathcal{B}$ in the reference configuration $\kappa_r(\mathcal{B})$. It is assumed that there exists a one-to-one mapping $\boldsymbol{\chi}$ such that at any time t it assigns the position $\mathbf{x} = \boldsymbol{\chi}(\mathbf{X}, t)$ to the particle X, in the current configuration $\kappa_t(\mathcal{B})$. The displacement field $\mathbf{u}$ is defined as:

$$\mathbf{u} = \mathbf{x} - \mathbf{X}. \tag{1}$$

The linearized strain tensor $\boldsymbol{\varepsilon}$ is defined by:

$$\boldsymbol{\varepsilon} = \frac{1}{2}\left(\nabla_{\mathbf{X}}\mathbf{u} + \nabla_{\mathbf{X}}\mathbf{u}^{\mathrm{T}}\right) \tag{2}$$

where $\nabla_{\mathbf{X}}$ is the gradient operator defined with respect to the reference configuration.

As we shall be interested in the deformations of a spherical body, it is most appropriate to refer quantities with respect to the spherical coordinate system. In the case of the spherical coordinates, where the displacement field has components u_r, u_θ, and u_ϕ, it follows from (2) that (see, for example, [7]):

$$\varepsilon_{rr} = \frac{\partial u_r}{\partial r}, \quad \varepsilon_{\theta\theta} = \frac{1}{r\sin\phi}\frac{\partial u_\theta}{\partial \theta} + \frac{u_r}{r} + \frac{u_\phi}{r}\cot\phi, \quad \varepsilon_{\phi\phi} = \frac{1}{r}\frac{\partial u_\phi}{\partial \phi} + \frac{u_r}{r}, \tag{3}$$

$$\varepsilon_{\phi\theta} = \frac{1}{2}\left(\frac{1}{r\sin\phi}\frac{\partial u_\phi}{\partial \theta} - \frac{u_\theta}{r}\cot\phi + \frac{1}{r}\frac{\partial u_\theta}{\partial \phi}\right), \quad \varepsilon_{\phi r} = \frac{1}{2}\left(\frac{1}{r}\frac{\partial u_r}{\partial \phi} - \frac{u_\phi}{r} + \frac{\partial u_\phi}{\partial r}\right), \tag{4}$$

$$\varepsilon_{\theta r} = \frac{1}{2}\left(\frac{\partial u_\theta}{\partial r} + \frac{1}{r\sin\phi}\frac{\partial u_r}{\partial \theta} - \frac{u_\theta}{r}\right). \tag{5}$$

If we assume that there are no body forces and if we consider quasi-static problems, the balance of linear momentum reduces to the equilibrium equation:

$$\operatorname{div}\mathbf{T} = \mathbf{0}. \tag{6}$$

On using spherical coordinates, Eq. (6) takes the form (see for instance [7]):

$$\frac{\partial T_{r\phi}}{\partial r} + \frac{1}{r}\frac{\partial T_{\phi\phi}}{\partial \phi} + \frac{1}{r\sin\phi}\frac{\partial T_{\theta\phi}}{\partial \theta} + \frac{3}{r}T_{r\phi} + \frac{\cos\phi}{r\sin\phi}(T_{\phi\phi} - T_{\theta\theta}) = 0, \tag{7}$$

$$\frac{\partial T_{r\theta}}{\partial r} + \frac{1}{r}\frac{\partial T_{\phi\theta}}{\partial \phi} + \frac{1}{r\sin\phi}\frac{\partial T_{\theta\theta}}{\partial \theta} + \frac{3}{r}T_{r\theta} + \frac{2}{r}\frac{\cos\phi}{\sin\phi}T_{\phi\theta} = 0, \tag{8}$$

$$\frac{\partial T_{rr}}{\partial r} + \frac{1}{r}\frac{\partial T_{\phi r}}{\partial \phi} + \frac{1}{r\sin\phi}\frac{\partial T_{\theta r}}{\partial \theta} + \frac{\cos\phi}{r\sin\phi}T_{r\phi} + \frac{1}{r}(2T_{rr} - T_{\phi\phi} - T_{\theta\theta}) = 0. \tag{9}$$

In this work, we consider the same nonlinear relation between the linearized strain tensor and the Cauchy stress tensor as in Part I [1] (see [9–11]) where the linearized strain is given by $\boldsymbol{\varepsilon} = \frac{\partial W}{\partial \mathbf{T}}$. For an isotropic body, we have $W = W(I_1, I_2, I_3)$, where

$$I_1 = \operatorname{tr}\mathbf{T}, \quad I_2 = \frac{1}{2}\operatorname{tr}\mathbf{T}^2, \quad I_3 = \frac{1}{3}\operatorname{tr}\mathbf{T}^3, \tag{10}$$

and in such a case we obtain

$$\boldsymbol{\varepsilon} = W_1\mathbf{I} + W_2\mathbf{T} + W_3\mathbf{T}^2, \tag{11}$$

where we have defined $W_i = \frac{\partial W}{\partial I_i}$, $i = 1, 2, 3$. The model (11) shares a feature in common with the classical linearized elastic model in that both of them are not Galilean invariant as the linearized strain is not Galilean invariant. Thus, the model should only be viewed as an approximation of the proper nonlinear models presented, for example, in [2–4,12,13].

Let us consider the particular expression for W presented in Part I [1], $W(I_1, I_2) = -\frac{\alpha}{\beta}\ln[\cosh(\beta I_1)] + \frac{\gamma}{\iota}\sqrt{1 + 2\iota I_2}$, where α, β, γ, and ι are constant. From (11), we obtain that

$$\boldsymbol{\varepsilon} = -\alpha\tanh(\beta I_1) + \frac{\gamma}{\sqrt{1 + 2\iota I_2}}\mathbf{T}. \tag{12}$$

Table 1 Values for the constants used in (12), (13)

α	β 1/Pa	γ 1/Pa	ι 1/Pa^2	E Pa	ν
0.01	9.27681×10^{-8}	4.01995×10^{-9}	10^{-14}	323387085	10.3

As in Part I [1], we are interested in comparing the results obtained for a boundary value problem within the context of (12), with the predictions of the classical constitutive equation for isotropic linearized elasticity:

$$\boldsymbol{\varepsilon} = -\frac{\nu}{E} I_1 \mathbf{I} + \frac{(\nu+1)}{E}\mathbf{T}. \tag{13}$$

We use the values for the constants in (12) and (13) presented in Table 1.

For more details concerning the choice of the values for the constants, see section 2.3 and figures 1 and 2 of Part I [1].

The following is the procedure we use to solve boundary value problems (see [1]): We appeal to a semi-inverse procedure and assume a simplified form for the stress tensor $\mathbf{T}$, which satisfies the equilibrium equation (6): $\operatorname{div}\mathbf{T} = \mathbf{0}$. Using the kinematic relation (2) and the above structure for the stress tensor, we solve the equation $\frac{1}{2}(\nabla\mathbf{u} + \nabla\mathbf{u}^{\mathrm{T}}) = \frac{\partial W}{\partial \mathbf{T}}$. This equation is solved to find simultaneously the components of the stress tensor and the displacement field.

3 Inflation of a sphere

Let us consider the sphere $r_{\mathrm{i}} \leq r \leq r_{\mathrm{o}}, 0 \leq \theta \leq 2\pi, 0 \leq \phi \leq \pi$ under the effect of a radial normal stress P_{i} applied on $r = r_{\mathrm{i}}$, assuming as well that there is no mechanical traction on the surface $r = r_{\mathrm{o}}$. Let us assume that the sphere is under the following state of stress: $\mathbf{T} = T_{rr}(r)\mathbf{e}_r \otimes \mathbf{e}_r + T_{\theta\theta}(r)\mathbf{e}_\theta \otimes \mathbf{e}_\theta + T_{\phi\phi}(r)\mathbf{e}_\phi \otimes \mathbf{e}_\phi$. It immediately follows from Eqs. (7) through (9) that:

$$\frac{\mathrm{d}T_{rr}}{\mathrm{d}r} + \frac{1}{r}(2T_{rr} - T_{\phi\phi} - T_{\theta\theta}) = 0, \quad \frac{\cos\phi}{r\sin\phi}(T_{\phi\phi} - T_{\theta\theta}) = 0, \tag{14}$$

which leads to

$$T_{\theta\theta} = T_{\phi\phi} = \frac{r}{2}\frac{\mathrm{d}T_{rr}}{\mathrm{d}r} + T_{rr}. \tag{15}$$

Let us assume that under such external loads the displacement field is of the form $\mathbf{u} = u_r(r)\mathbf{e}_r$; then, from (3)–(5), we obtain the following components of the linearized strain tensor:

$$\varepsilon_{rr} = \frac{\mathrm{d}u_r}{\mathrm{d}r}, \quad \varepsilon_{\theta\theta} = \varepsilon_{\phi\phi} = \frac{u_r}{r}, \quad \varepsilon_{r\theta} = \varepsilon_{r\phi} = \varepsilon_{\theta\phi} = 0. \tag{16}$$

From (11), we obtain two (in general nonlinear) ordinary differential equations for $u_r(r)$ and $T_{rr}(r)$:

$$\frac{\mathrm{d}u_r}{\mathrm{d}r} = W_1 + W_2 T_{rr} + W_3 T_{rr}^2, \tag{17}$$

$$\frac{u_r}{r} = W_1 + W_2\left(\frac{r}{2}\frac{\mathrm{d}T_{rr}}{\mathrm{d}r} + T_{rr}\right) + W_3\left(\frac{r}{2}\frac{\mathrm{d}T_{rr}}{\mathrm{d}r} + T_{rr}\right)^2 \tag{18}$$

where W_i, $i = 1, 2, 3$ depend in general on the invariants (10), which in this case are given as:

$$I_1 = r\frac{\mathrm{d}T_{rr}}{\mathrm{d}r} + 3T_{rr}, \tag{19}$$

$$I_2 = \frac{3}{2}T_{rr}^2 + \frac{r^2}{4}\left(\frac{\mathrm{d}T_{rr}}{\mathrm{d}r}\right)^2 + rT_{rr}\frac{\mathrm{d}T_{rr}}{\mathrm{d}r}, \tag{20}$$

$$I_3 = T_{rr}^3 + \frac{r^3}{12}\left(\frac{\mathrm{d}T_{rr}}{\mathrm{d}r}\right)^3 + \frac{r^2}{2}T_{rr}\left(\frac{\mathrm{d}T_{rr}}{\mathrm{d}r}\right)^2 + rT_{rr}^2\frac{\mathrm{d}T_{rr}}{\mathrm{d}r}. \tag{21}$$

Table 2 Cases to be considered for the sphere

Outer radius r_o (m)	Maximum inner normal radial stress P_{max} (Pa)
0.11	5×10^6
0.2	8.8×10^6
100	10^7

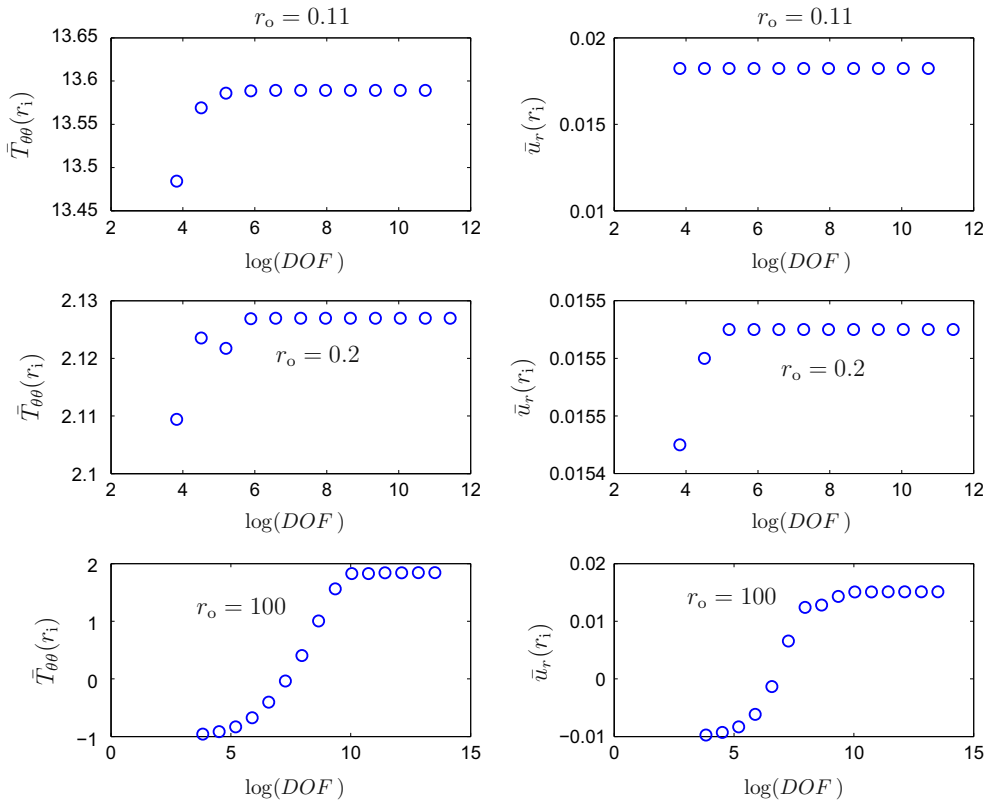

Fig. 1 Influence of the mesh density for the three examples of spheres presented in Table 2. Results for the dimensionless azimuthal stress $\bar{T}_{\theta\theta} = T_{\theta\theta}/P_i$ and the dimensionless displacement $\bar{u}_r = u_r/r_i$ evaluated at $r = r_i$ versus the natural logarithm of degrees of freedom DOF

The boundary conditions to be satisfied are:

$$T_{rr}(r_i) = -P_i, \quad T_{rr}(r_o) = 0. \tag{22}$$

When we consider the classical model (13), the Eqs. (17), (18) become linear differential equations, whose well-known solutions [considering (22)] are (see, for example, Chapters XV and XVI of [14]):

$$T_{rr}(r) = \frac{P_i r_i^3 (r_o^3 - r^3)}{r^3 (r_i^3 - r_o^3)}, \quad T_{\theta\theta}(r) = -\frac{P_i r_i^3 (2r^3 + r_o^3)}{2r^3 (r_i^3 - r_o^3)}, \tag{23}$$

$$u_r(r) = \frac{P_i r_i^3 [r^3(4\nu - 2) - r_o^3(1 + \nu)]}{2Er^2 (r_i^3 - r_o^3)}. \tag{24}$$

In the case of the new class of models (12), we have been unable to obtain exact solutions for (17), (18). In order to obtain approximate solutions, we use the finite element method, for which we manipulated the general Eqs. (17), (18) further. It is easy to show that (17) and (18) can be reduced to the nonlinear second order ordinary differential equation (for $T_{rr}(r)$):

$$\frac{\mathrm{d}}{\mathrm{d}r}\left\{ r\left[W_1 + W_2\left(\frac{r}{2}\frac{\mathrm{d}T_{rr}}{\mathrm{d}r} + T_{rr}\right) + W_3\left(\frac{r}{2}\frac{\mathrm{d}T_{rr}}{\mathrm{d}r} + T_{rr}\right)^2\right]\right\} = W_1 + W_2 T_{rr} + W_3 T_{rr}^2. \tag{25}$$

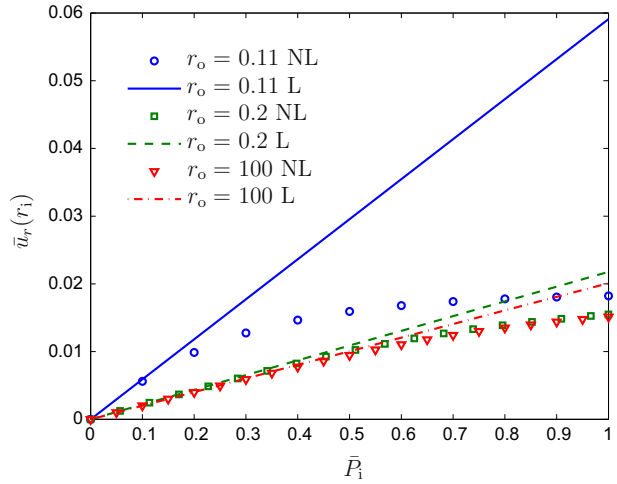

Fig. 2 Variation of the dimensionless radial displacement $\bar{u}_r = u_r/r_i$ evaluated at $r = r_i$ vs the dimensionless inner radial normal stress $\bar{P}_i = P_i/P_{max}$ for the three examples of spheres documented in Table 2, where P_{max} is the maximum inner radial normal stress, which for each sphere is also presented in Table 2. 'NL' means that the results are obtained considering (12) using the finite element method. 'L' refers to the results obtained considering (13) [see (24)]

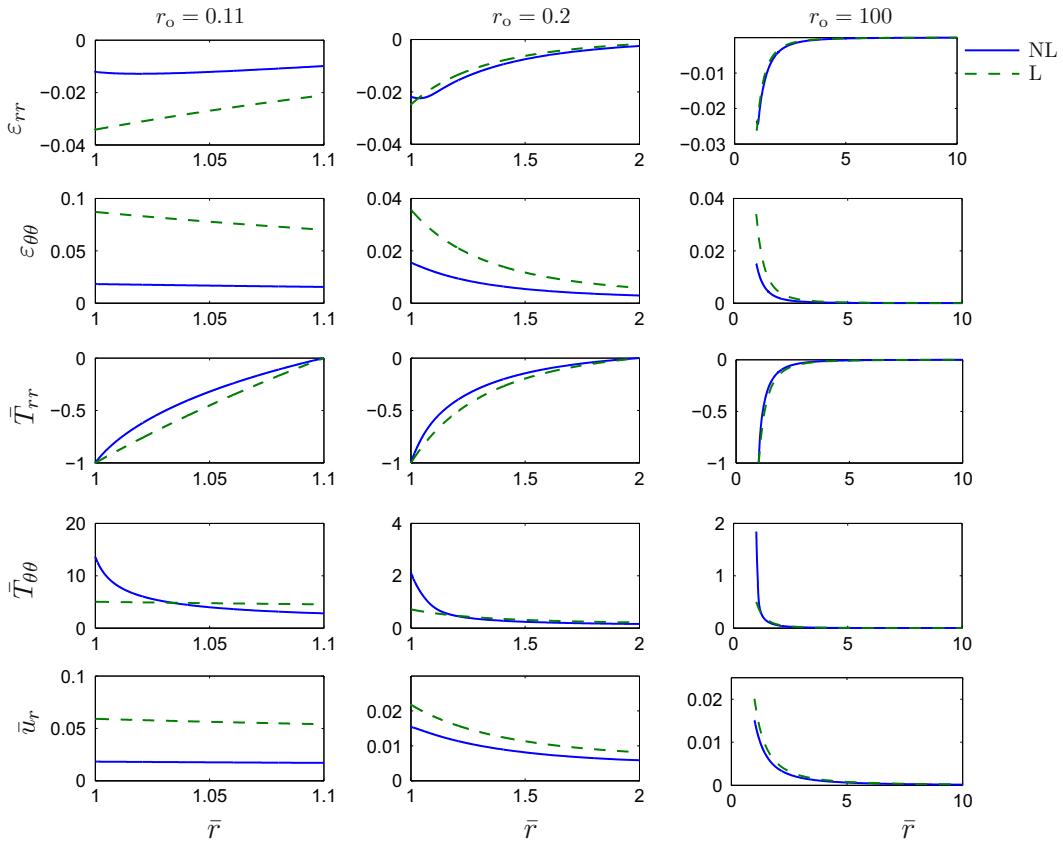

Fig. 3 From top to bottom: distributions of radial and circumferential components of the strain tensor, dimensionless radial and circumferential components of the stress tensor and dimensionless radial displacement, as functions of the dimensionless radial position $\bar{r} = r/r_i$, for the three examples of spheres presented in Table 1 ($r_o = 0.11$, $r_o = 0.2$, $r_o = 100$), comparing the results between the constitutive relation (12) (NL), and the results obtained for the classical linearized elastic bodies (13) (L) [see (23), (24)]

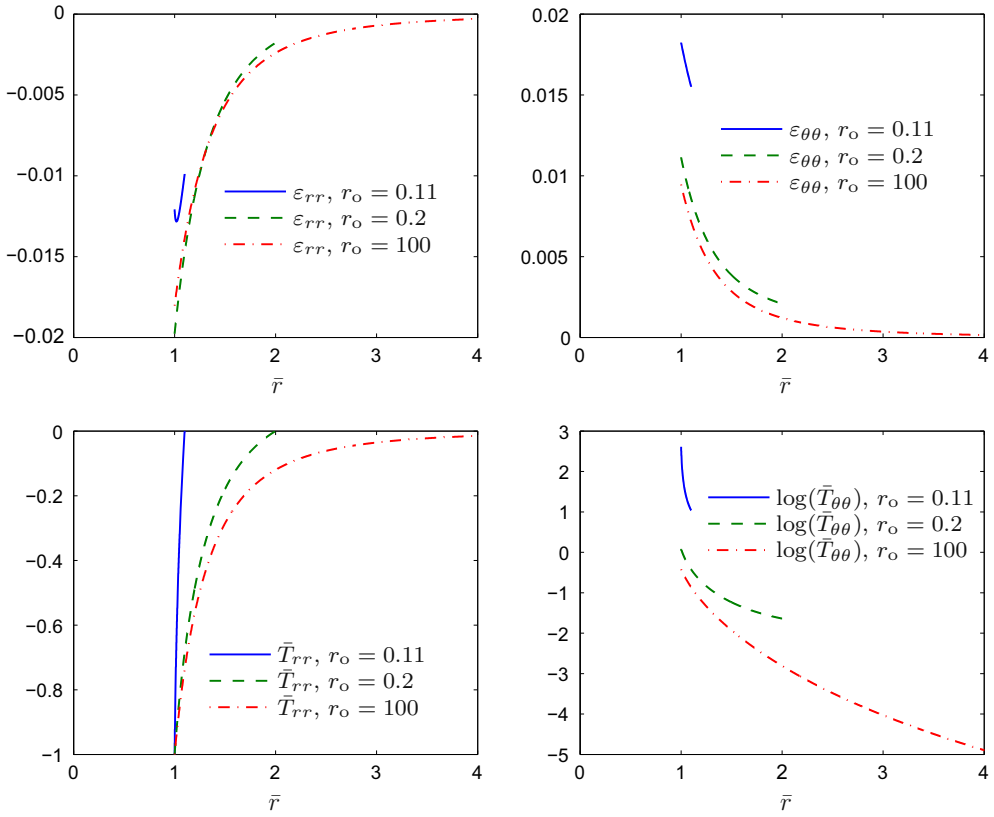

Fig. 4 Distributions of strains and dimensionless stresses, comparing the response of the three spheres considered in Table 2 and using (12), as functions of the dimensionless radial position $\bar{r} = r/r_i$. The inner radial normal stress for the three cases is $P_i = 5 \times 10^6$ Pa

If we define $\Gamma = r\left[W_1 + W_2\left(\frac{r}{2}\frac{dT_{rr}}{dr} + T_{rr}\right) + W_3\left(\frac{r}{2}\frac{dT_{rr}}{dr} + T_{rr}\right)^2\right]$ and $F = W_1 + W_2 T_{rr} + W_3 T_{rr}^2$, then Eq. (25) takes the form $\frac{d\Gamma}{dr} = F$, which can be solved using the finite element method in conjunction with the Newton method as we did for the problems for a tube that was presented in Part I of this work [1].

Three examples are considered for the sphere, where the external radii are different, but the internal radius $r_i = 0.1$m is the same. These three cases are presented in Table 2.

For each case, we list the maximum normal radial stress P_i that was possible to be applied without having problems with regard to the convergence of the code. The first case would represent a hollow sphere with a 'thin' wall, while the third case would correspond, approximately, to the case of an 'infinite' medium with a spherical void under the effect of a radial normal stress. The equation is solved using the finite element program Comsol 4.2 [15].

In the different plots to be presented in this section, we use the following dimensionless quantities:

$$\bar{r} = \frac{r}{r_i}, \quad \bar{T}_{rr} = \frac{T_{rr}}{P_i}, \quad \bar{T}_{\theta\theta} = \frac{T_{\theta\theta}}{P_i}, \quad \bar{u}_r = \frac{u_r}{r_i}, \quad \bar{P}_i = \frac{P_i}{P_{max}}. \tag{26}$$

In Fig. 1, we display the influence of the mesh density for the three different examples of spheres presented in Table 2, when solving (25) with the finite element method. In the figure, we display the variation of the dimensionless azimuthal stress through the thickness of the annulus and the dimensionless radial displacement evaluated at $r = r_i$, for different mesh densities, which are presented as functions of the natural logarithm of the degrees of freedom.

In Fig. 2, we present results for the three spheres defined in Table 2, depicting the radial dimensionless displacement evaluated at the inner radius vs the dimensionless inner normal radial stress $\bar{P}_i$. We compare these results with the results obtained for the classical linearized bodies.

In Fig. 3, we present results for the distribution of stresses, strains, and displacement in the dimensionless radial direction, ensuring that the maximum internal normal radial stress does not exceed the value mentioned in Table 2, i.e., for the sphere $r_o = 0.11$ m when $P_i = 5 \times 10^6$ Pa, for the sphere $r_o = 0.2$ m when $P_i = 8, 8 \times 10^6$ Pa, and finally for the sphere $r_o = 100$ m when $P_i = 10^7$ Pa. For each plot, there is a comparison between the results obtained for the constitutive Eq. (12), using the finite element method (NL), and the results obtained using (13) from (23), (24) for the classical linearized elastic model (L). For the sphere $r_o = 100$ m, the results are only presented for the range $1 \leq \bar{r} \leq 15$, not for the whole wall thickness $1 \leq \bar{r} \leq 1000$.

Finally, in Fig. 4, a comparison is provided between the response of the three spheres (see Table 2), when the constitutive relation (12) is considered. The internal radial normal stress P_i is the same for the three cases and equals 5×10^6 Pa.

Acknowledgments R. Bustamante would like to express his gratitude for the financial support provided by FONDECYT (Chile) under Grant No. 1120011. K. R. Rajagopal thanks the National Science Foundation and the Office of Naval Research for support of this work.

References

1. Bustamante, R., Rajagopal, K.R.: Solutions of some boundary value problems for a new class of elastic bodies undergoing small strains. Comparison with the predictions of the classical theory of linearized elasticity: Part I problems with cylindrical symmetry. Acta Mech. (2014). doi:10.1007/s00707-014-1293-z
2. Rajagopal, K.R.: On implicit constitutive theories. Appl. Math. **48**, 279–319 (2003)
3. Rajagopal, K.R.: The elasticity of elasticity. Z. Angew. Math. Phys. **58**, 309–317 (2007)
4. Rajagopal, K.R.: Conspectus of concepts of elasticity. Math. Mech. Solids **16**, 536–562 (2011)
5. Rajagopal, K.R.: Rethinking constitutive theories (Submitted)
6. Chadwick, P.: Continuum Mechanics: Concise Theory and Problems. Dover Publications INC, Mineola (1999)
7. Saada, A.S.: Elasticity: Theory and Application. Krieger Publishing Company, Malabar (1993)
8. Truesdell, C.A., Toupin, R.: The classical field theories. In: Handbuch der Physik, vol. III/1. Springer, Berlin (1960)
9. Bustamante, R.: Some topics on a new class of elastic bodies. Proc. R. Soc. A **465**, 1377–1392 (2009)
10. Ortiz, A., Bustamante, R., Rajagopal, K.R.: A numerical study of a plate with a hole for a new class of elastic bodies. Acta Mech. **223**, 1971–1981 (2012). doi:10.1007/s00707-012-0690-4
11. Ortiz-Bernardin, A., Bustamante, R., Rajagopal, K.R.: A numerical study of elastic bodies that are described by constitutive equations that exhibit limited strains. Int. J. Solids Struct. **51**, 875–885 (2014)
12. Rajagopal, K.R., Srinivasa, A.R.: On a class of non-dissipative solids that are not hyperelastic. Proc. R. Soc. A **465**, 493–500 (2009)
13. Rajagopal, K.R: On the nonlinear elastic response of bodies in the small strain range. Acta Mech. **225**, 1545–1553 (2014)
14. Lamé, M.G.: Leşons sur la Théorie Mathématique de L'Élasticité des Corps Solides. Deuxième Édition, Paris, Gauthier-Villars (1866)
15. Comsol Multiphysics, Version 3.4, Comsol Inc. Palo Alto, CA (2007)